JACS
JOURNAL OF THE AMERICAN CHEMICAL SOCIETY
Article
pubs.acs.org/JACS

Elucidating the Role of Site-Specific Nitration of α-Synuclein in the Pathogenesis of Parkinson's Disease via Protein Semisynthesis and Mutagenesis

Ritwik Burai, Nadine Ait-Bouziad, Anass Chiki, and Hilal A. Lashuel*

Laboratory of Molecular and Chemical Biology of Neurodegeneration, Brain Mind Institute, Ecole Polytechnique Fédérale de Lausanne (EPFL), CH-1015 Lausanne, Switzerland

Supporting Information

ABSTRACT: Parkinson's disease (PD) is characterized by the loss of dopaminergic neurons in the *substantia nigra* and the presence of intraneuronal inclusions consisting of aggregated and post-translationally modified α-synuclein (α-syn). Despite advances in the chemical synthesis of α-syn and other proteins, the generation of site-specifically nitrated synthetic proteins has not been reported. Consequently, it has not been possible to determine the roles of nitration at specific residues in regulating the physiological and pathogenic properties of α-syn. Here we report, for the first time, the site-specific incorporation of 3-nitrotyrosine at different regions of α-syn using native chemical ligation combined with a novel desulfurization strategy. This strategy enabled us to investigate the role of nitration at single or multiple tyrosine residues in regulating α-syn structure, membrane binding, oligomerization, and fibrils formation. We demonstrate that different site-specifically nitrated α-syn species exhibit distinct structural and aggregation properties and exhibit reduced affinity to negatively charged vesicle membranes. We provide evidence that intermolecular interactions between the N- and C-terminal regions of α-syn play critical roles in mediating nitration-induced α-syn oligomerization. For example, when Y39 is not available for nitration (Y39F and Y39/125F), the extent of cross-linking is limited mostly to dimer formation, whereas mutants in which Y39 along with one or multiple C-terminal tyrosines (Y125F, Y133F, Y136F and Y133/136F) can still undergo nitration readily to form higher-order oligomers. Our semisynthetic strategy for generating site-specifically nitrated proteins opens up new possibilities for investigating the role of nitration in regulating protein structure and function in health and disease.

INTRODUCTION

Among the various protein post-translational modifications (PTMs) occurring in cells, oxidative and nitrative modifications are of major importance and have been implicated in normal aging and the pathogenesis of several neurodegenerative disorders.[1−3] Nitration is a consequence of elevated oxidative stress, which is recognized as one of the major factors contributing to neuronal injury and cell degeneration in neurodegenerative diseases. Oxidative stress leads to the generation of reactive nitrative species, such as peroxynitrite ($ONOO^-$), which is produced by the reaction between superoxide ($O_2^{-\bullet}$) and nitric oxide radical ($NO^\bullet$).[4,5] Under certain conditions, peroxynitrite further degrades to the very reactive nitrogen dioxide radical ($NO_2^\bullet$), which directly reacts with tyrosine residues in proteins to form 3-nitrotyrosine (3-NT)[6] (Figure 1A). The reaction between tyrosine and peroxynitrite can also result in dityrosine formation via an o,o′-dityrosine bond,[6] which leads to the formation of stable protein oligomers, including dimers, trimers, and higher oligomeric species (Figure 1A).

Several lines of evidence suggest that protein nitration plays an important role in the pathogenesis of neurodegenerative disorders. (1) Increased 3-NT immunostaining has been reported in Lewy bodies (LBs), Lewy neurites (LNs), and glial cytoplasmic inclusions (GCIs) isolated from patients affected with PD or other related synucleinopathies, such as dementia with Lewy bodies (DLB), multiple system atrophy (MSA), and Lewy body variant of Alzheimer's diseases (LBVAD).[7,8] (2) Immunostaining has revealed copious amount of nitrated α-syn

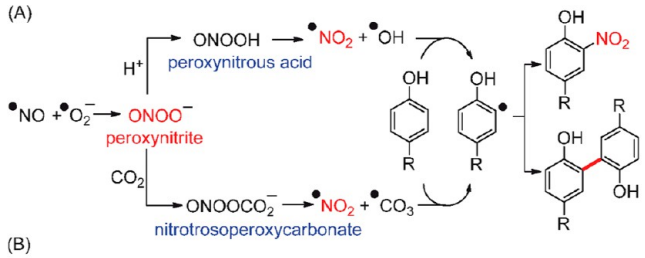

Figure 1. Free radical pathways of tyrosine nitration and dityrosine formation. (A) *In vivo* pathways of peroxynitrite-mediated protein nitration and cross-linking. (B) Nitration sites of *a*-syn.

Received: December 29, 2014
Published: March 13, 2015

DOI: 10.1021/ja5131726
J. Am. Chem. Soc. 2015, 137, 5041−5052

Scheme 1. Schematic Depiction of the Different Approaches Used to Generate Non-Specific and Site-Specific Nitrated α-Synuclein[a]

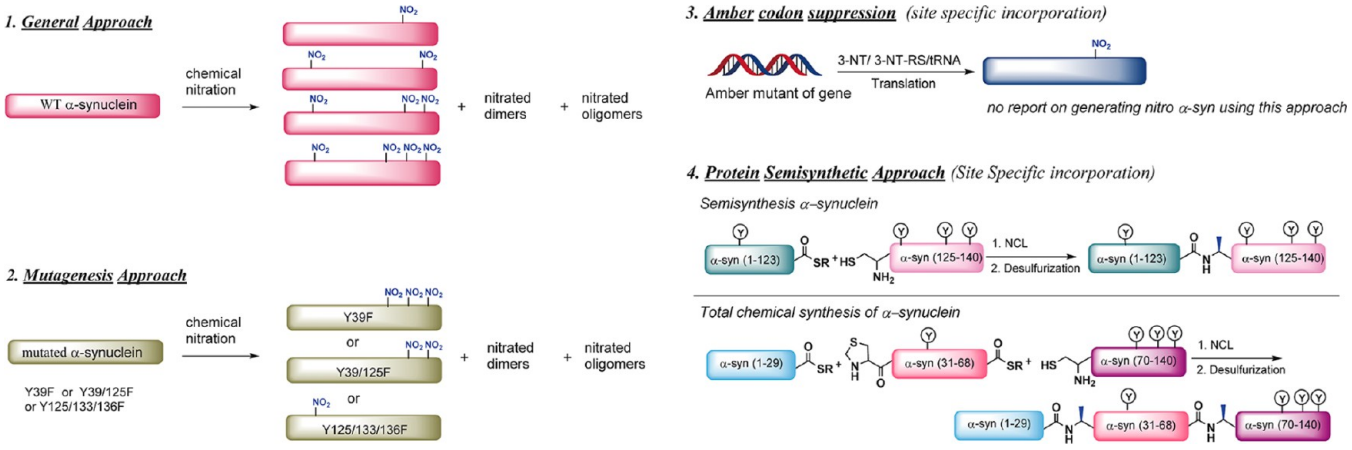

[a]Non site-specific chemical nitration (left panel). Site-specific chemical nitration requires mutagenesis (left panel). Site-specific incorporation of 3-NT in a protein using the amber suppression codon technique (right top panel). A semisynthetic strategy allows efficient site-specific introduction of 3-NT in α-syn (bottom right panel).

Scheme 2. Synthetic Strategy and Standard/Modified Desulfurization Conditions Used to Generate Site-Specific Nitro α-syn[a]

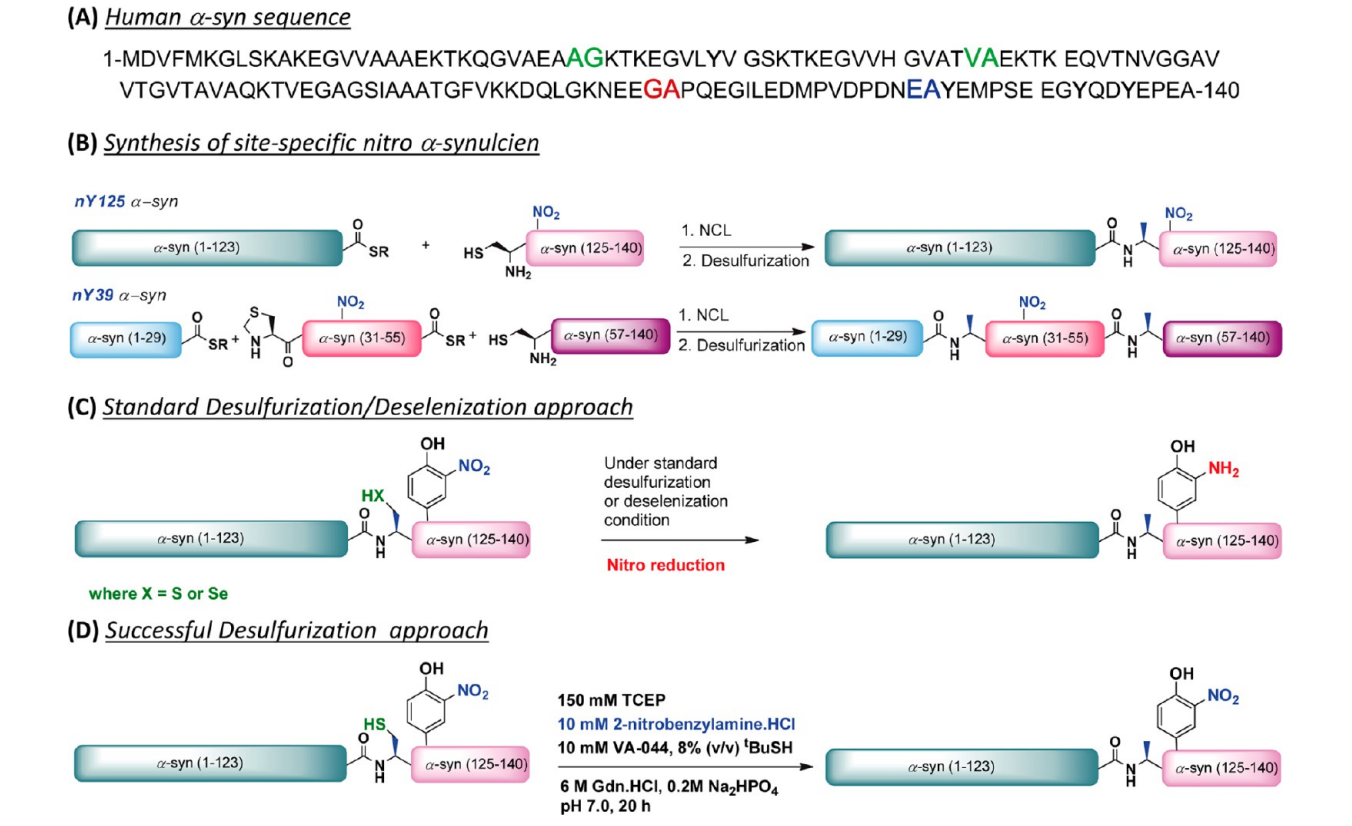

[a](A) Human α-syn sequence showing the ligation sites used in the generation of synthetic and semisynthetic α-syn using native chemical ligations: G106-A107 (red), new ligation site E123-A124 (blue), and A29-G30, V55-A56 (green). (B) Synthetic strategy to generate nitro α-syn. (C) Standard desulfurization/deselenization approaches. (D) 2-nitrobenzylamine hydrochloride salt slows down the nitro reduction and enables cysteine desulfurization in the presence of 3-NT.

in pathological lesions of patients suffering from diverse synucleinopathies.[7,8] (3) Nitrated forms of α-syn have been detected in the sera[9] and peripheral blood mononuclear cells of patients with PD,[10] suggesting that the α-syn nitration profile could be used as a PD biomarker or therapeutic target. (4) A mixture of nitrated α-syn species (monomers, dimers, trimers, and oligomers, but not the isolated nitrated α-syn monomers) is significantly more toxic to SHSY-5Y cells[11,12] and primary neurons[12] than WT α-syn and induces loss of dopaminergic neurons upon administration in the *substantia nigra pars compacta* of rats.[12] (5) Nitrated α-syn fibrils stimulate microglial cells and activate their neurotoxic inflammatory phenotype,

DOI: 10.1021/ja5131726
J. Am. Chem. Soc. 2015, 137, 5041−5052

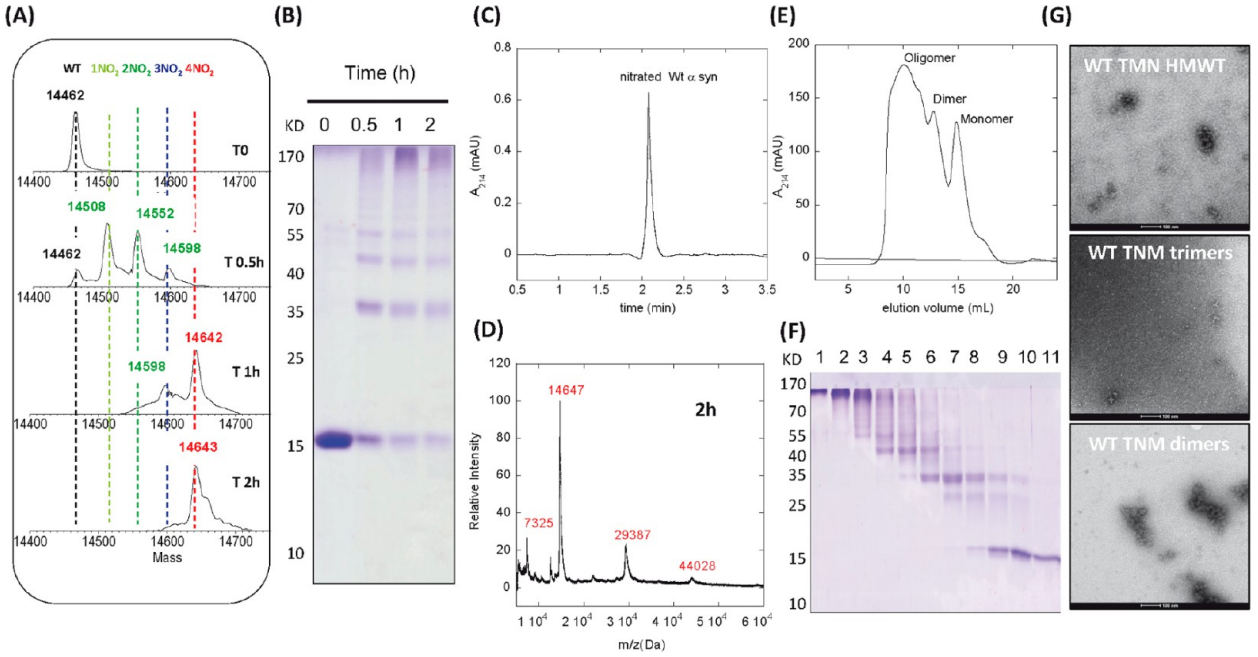

Figure 2. Nitration of WT α-syn using TNM. (A) Nitration reaction kinetics were monitored by ESI-LC/MS. (B) SDS-PAGE. Lanes 1−4 represent the reaction after 0, 0.5, 1, and 2 h, respectively. (C) RP-UPLC of nitrated WT α-syn. (D) MALDI-TOF analysis of nitrated WT α-syn after 2 h (expected tetra-nitrated mass: 14 642 Da $[M + H]^+$). (E) Size exclusion chromatogram and (F) corresponding SDS-PAGE of SEC fractions. (G) Electron micrographs of recombinant nitrated WT α-syn species. The scale bars are 100 nm.

which accelerates the degeneration of dopaminergic neurons.[13] (6) Finally, induction of nitrative insult following exposure to oxidizing and nitrating species or nitric oxide synthase overexpression induces α-syn nitration and aggregation in HEK 293[14] and inclusion formation[15] in differentiated PC12 cells.[16] Taken together, this body of data suggests that nitration of α-syn significantly alters its biochemical, biophysical, and cellular properties and may contribute to the pathology of PD, possibly through promotion of α-syn oligomerization and/or fibrillogenesis.

Human α-syn possesses four tyrosine residues: one located in the N-terminal region at position 39 and three others in the C-terminal region at positions 125, 133, and 136 (Figure 1B). These residues are all susceptible to oxidative stress-related nitration.[8] Several studies have attempted to elucidate the effect of tyrosine nitration on α-syn cellular properties by assessing the effects of α-syn tyrosine nitration on aggregation, vesicle binding, proteolytic degradation, microglia activation, and neurotoxicity.[17−19] Nitration of α-syn was shown to promote the formation of partially folded states[17] and stable oligomeric species that do not go on to form α-syn fibrils.[17,18,20] Addition of isolated nitrated monomers and dimers was shown to accelerate the rate of WT α-syn fibrilization when present in low amounts, whereas oligomers inhibit WT α-syn fibrilization.[19] Nitration also results in decreased affinity of α-syn for lipid membranes through electrostatic repulsion in the case of Y39 nitrated α-syn[19,21] and conformational alteration of C-terminally (Y125, Y133 and Y136) nitrated forms of the protein.[21] However, the majority of these studies were performed under nonchemoselective conditions leading to nonspecific nitration of all tyrosine residues, resulting in the formation of heterogeneous mixtures of α-syn species with different nitration patterns and levels of nitration at each residue as well as different oligomeric species. Indeed, *In vitro* exposure of α-syn to peroxynitrite/CO_2,[15,19,20,22,23] H_2O_2/sodium nitrite/myeloperoxidase,[20] 3-morpholinosydnonimine (SIN-1),[12] tetranitromethane (TMN),[17,18,21] or $NaNO_2$[11] results not only in mixtures of mono, di, tri, and tetra-nitrated proteins at different sites but also leads to the formation of o,o′-dityrosine cross-linked dimers, trimers, and higher oligomeric species, with all possible dityrosine cross-linking combinations.[17,18,20]

To address these limitations and to elucidate the role of nitration at single or specific combinations of nitration sites, tyrosine residues are often mutated to phenylalanine, excluding the desired tyrosine residue(s) (Scheme 1). However, the introduction of Y → F mutations likely alters a protein's biochemical, biophysical, and cellular properties, particularly in proteins that contain multiple tyrosine residues, such as α-syn. Theoretically, site-specifically nitrated forms of α-syn can be obtained using the amber suppression codon technique, in which 3-NT residues are incorporated site-specifically using 3-NT specific aminoacyl-tRNA synthetase/cognate tRNA pairs (Scheme 1).[24] However, the high level of protein truncations and the poor yield associated with the incorporation of more than one 3-NT limit the utility of this approach. Interestingly, Danielson et al. demonstrated that endogenous α-syn could be preferentially nitrated at Y39 by overexpressing monoamine oxidase B (MAO-B), albeit with a very low level of nitration (1%).[25]

Here, we report a general and efficient semisynthetic strategy that permits for the first time the site-specific introduction of 3-NT into proteins (Scheme 1) using native chemical ligation followed by modified desulfurization conditions that prevent nitro reduction (Scheme 2). This strategy was then successfully applied to the production of milligram quantities of α-syn nitrated selectively at Y39 or Y125, allowing detailed biophysical and biochemical studies of the effect of site-specific tyrosine nitration on α-syn structure, oligomerization, and fibril formation. Herein, we present an experimental approach that illustrates how combining protein semisynthesis, mutagenesis,

DOI: 10.1021/ja5131726
J. Am. Chem. Soc. 2015, 137, 5041−5052

Scheme 3. Semisynthesis and Characterization of nY125 α-syn[a]

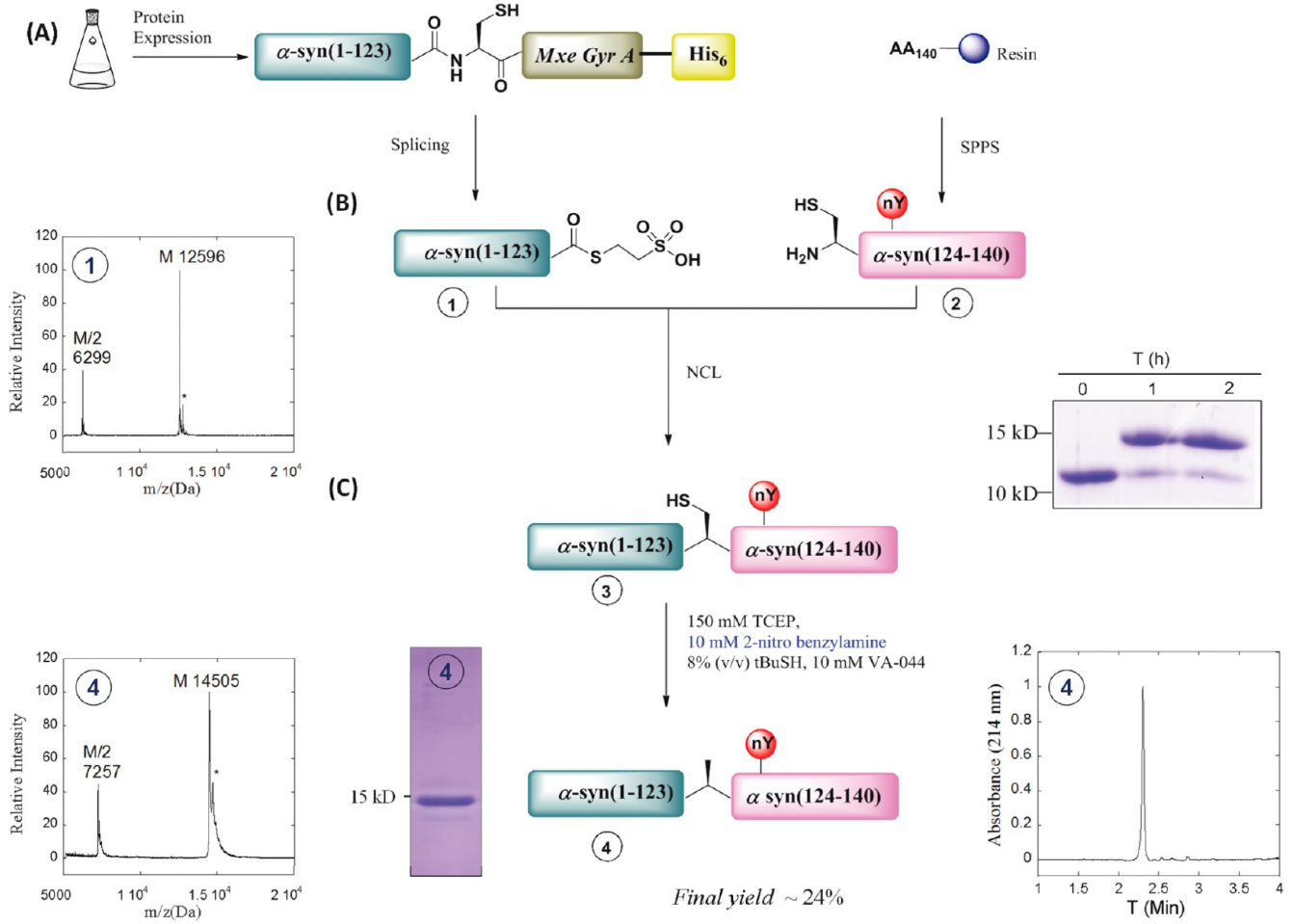

[a](A) Expressed protein ligation (EPL) approach used to generate nY125 α-syn. The thioester fragment **1** was generated using intein-mediated thioester formation. MALDI-TOF analysis of **1** (expected mass: 12 595 Da $[M + H]^+$). The synthetic peptide **2** was generated by Fmoc-based SPPS. LCMS analysis of **2**. (B) Full-length semisynthetic **3** was generated by NCL between **1** and **2**. SDS-PAGE analysis confirmed the NCL reaction; lanes 1, 2, and 3 represent the ligation reaction at 0, 1, and 2 h, respectively. (C) Desulfurization of **3** to generate nY125 α-syn **4**. SDS-PAGE, MALDI-TOF and RP-UPLC analyses of **4** (expected mass: 14 506 Da $[M + H]^+$; * corresponds to sinapinic adduct) confirming the purity of the final purified product.

and chemical-mediated nitration advances our understanding of the role of nitration and other post-translational modifications in regulating protein structure, function, and activity in health and disease.

RESULTS AND DISCUSSION

Nitration of WT α-syn Results in the Formation of a Mixture of Nitrated Monomers and Dityrosine Cross-Linked Nitrated Species. To determine the effect of nitration at all tyrosine residues, recombinant human WT α-syn was treated with TNM, and the extent of nitration was monitored by matrix-assisted laser desorption ionization time-of-flight (MALDI-TOF) and electrospray ionization liquid chromatography mass spectrometry (ESI-LC/MS). Sevcisk et al.[21] previously demonstrated that treatment of WT α-syn with TNM resulted in the formation of 15%, 35%, 35%, and 15% of mono, di, tri, and tetra-nitrated α-syn, respectively, along with other cross-linked species. Therefore, to generate fully tetra-nitrated α-syn, we incubated WT α-syn with 40 equiv of 10% ethanolic TNM at pH 8.1, and when necessary, an additional 40 equiv of 10% ethanolic TNM was added after 30 min to push the reaction to completion. Under these conditions, complete nitration of all four tyrosines was achieved within 2 h at 30 °C (Figure 2A). MALDI-TOF and SDS-PAGE analyses of the reaction revealed the formation of mono-, di-, tri-, and tetra-nitrated α-syn species, in addition to high molecular weight species and the disappearance of the monomer over time (Figure 2B,D). The mixture of oligomers eluted as a single peak on reversed-phase ultraperformance liquid chromatography (RF-UPLC) (Figure 2C). To characterize the different oligomeric species, the TNM-nitrated α-syn mixture was injected into a Superdex 200 10/300 GL size exclusion chromatography (SEC) column. SDS-PAGE analysis of the SEC fractions revealed a reasonable separation of α-syn monomers (lanes 11−9), dimers (lanes 8−7), and higher order aggregates (lanes 6−1) (Figure 2E,F). Characterization of these fractions by transmission electron microscopy (TEM) revealed the presence heterogeneous oligomeric species in all cases (Figure 2G).

Site-Specific Nitration of α-syn Using Expressed Protein Ligation. In contrast to phosphorylation, no enzymes are known to regulate α-syn nitration *in vivo*, and no natural amino acids can mimic nitro tyrosine. To address these

DOI: 10.1021/ja5131726
J. Am. Chem. Soc. 2015, 137, 5041−5052

limitations, we developed a semisynthetic strategy that enables site-specific nitration of α-syn (Scheme 2B). We previously reported the generation of homogeneously phosphorylated (S129 and Y125), acetylated, and mono-, di-, and tetra-ubiquitinated α-syn using total chemical synthesis and semisynthesis approaches.[26−28] Subsequently, the Petersson group also used similar strategies to generate semisynthetic thioamide α-syn for FRET studies.[29] Because three of the four tyrosine residues are within the last C-terminal 20 residues (Y125, Y133, and Y136), we applied a semisynthetic strategy similar to the one we recently reported to generate α-syn phosphorylated at Y125,[26] with the ligation site moved from residues G106-A107 to E123-A124 (Scheme S1). As the native sequence of α-syn does not contain any cysteine residues (Scheme 2A), we mutated A124 to C124 to perform the NCL reaction. To recover the native sequence, desulfurization of the cysteine to an alanine is necessary.

Prior to this study, there were no reports on the semisynthesis of nitrated proteins, most likely because the standard desulfurization conditions result in the reduction of the nitro group. Indeed, when a nitro-protein is subjected to standard desulfurization conditions (0.5 M TCEP, 10 mM VA-044, and 8% (v/v) ^{t}BuSH in 6.0 M Gdn·HCl, 0.2 M Na_2HPO_4), both NO_2 group reduction to an amino group ($-NH_2$) and desulfurization of the cysteine residue (Scheme 2C) are observed. The reaction kinetic of nitro reduction (via radical pathways) competes with the radical-mediated cysteine desulfurization, most likely because the aryl NO_2 group is amenable to reduction under radical desulfurization conditions. We attempted to avoid the undesired nitro reduction by using selenocysteine-mediated ligation. We hypothesized that the mild and increased rate of deselenization might result in sufficiently short reaction times to eliminate undesired side reactions. The selenocysteine nitro peptide was ligated faster (<1 h) and led to high yields (<95% conversion of α-syn(1−123)SR to ligated product), as assessed by SDS-PAGE analysis (Figure S6E). Inspired by the deselenization conditions reported by Dawson's group,[30] we attempted to deselenize the nY125-α-syn-124U protein. Despite screening several conditions, we failed to identify conditions that led to efficient desulfurization/deselenization and prevented reduction of the nitro group (Table S1). This result can be explained by the high propensity of selenium to form radicals, which also drive nitro reduction via radical-mediated mechanisms.[30]

To avoid using a radical-based desulfurization process, we explored the possibility of using the cysteine-based electron-rich thio-benzyl auxiliary, which has been successfully used by Danishefsky and co-workers[31] to ligate two glycopeptides at the Gly-Ala site. In our case, *trans*-thioesterification between the thioester and cys auxiliary occurred within 1 h, but the rate-determining acyl transfer step was sluggish compared to the hydrolysis of the intermediate thioester (Figure S7). The insolubility of the thioester in aprotic solvent, such as DMSO and DMF, limited the utility of this approach.

We envisioned that the presence of additional NO_2 groups in the reaction buffer might decrease the probability of 3-NT reduction in the protein. We chose 2-nitrobenzylamine hydrochloride because of its water solubility. We observed that the addition of 10 mM 2-nitrobenzylamine hydrochloride salt with 150 mM TCEP, 10 mM VA-044, and 8% (v/v) ^{t}BuSH significantly slowed the nitro reduction and allowed the generation of desulfurized 3-NT α-syn (Scheme 2, D), although the exact mechanism underlying the effects of 2-nitrobenzylamine is unknown. The kinetics of desulfurization were followed by ESI-LC/MS, and a loss of mass of −32 Da mass loss (Figure S8) was observed. Up to 18 h, no nitro reduction was detectable by ESI-LC/MS, while 15%−20% of the starting material remained unreacted. Attempts to push the reaction to completion led to increased nitro reduction, methionine oxidation, and TCEP-mediated cleavage of the ligated product.[32]

Semisynthesis of α-syn Nitrated at Y125. Having established an efficient desulfurization strategy, we next focused on producing semisynthetic full-length α-syn nitrated at Y125. Recombinant α-syn(1−123)SR was expressed in *E. coli* using an engineered mini-intein (*Mxe GyrA*), which exploits the mechanism of intein self-splicing to generate recombinant proteins with a C-terminal thioester in the presence of thiol (Scheme 3A).[33] In brief, truncated α-syn(1−123) was expressed in fusion with the GyrA mini-intein (*Mxe GyrA*) which contains a C-terminal hexa-histidine purification tag to facilitate its purification from bacterial lysates. The cell lysates were passed through a Ni-NTA column to purify the fusion protein from undesired proteins. The fusion protein was then spliced with excess sodium 2-mercaptoethanesulfonate (0.25 M) to obtain the α-syn(1−123)SR. The protein thioester was then purified by RP-HPLC and characterized by MALDI-TOF and RP-UPLC (Scheme 3A and Figure S2).

The peptide comprising residues 124−140 and containing an N-terminal cysteine and the nitrated amino acid was prepared by solid-phase peptide synthesis using commercially available Fmoc-protected 3-nitro tyrosine (Aldrich) (Figure S1). Recently, the Kent group[34] reported native chemical ligation at the Glu-Cys site without any side reaction using mercaptophenyl acetic acid (MPAA) as a catalyst. Consistent with their findings, we observed rapid (2 h) and efficient ligation of the α-syn(1−123)SR and the nY125 α-syn (A124C-140) peptide when using MPAA as a catalyst. The ligation was monitored by SDS-PAGE and ESI-LC/MS, which revealed a single band and a peak at 14 533 Da (expected mass: 14 537 Da $[M + H]^+$, Scheme 3B), respectively. The reaction rate was similar to that of the WT α-syn synthesis at this particular site, with 90% conversion after 2 h (Figures S3 and S4). Interestingly, we observed that α-syn(1−123)SR was more resistant to hydrolysis than α-syn(1−106)SR. After removal of the catalyst using a PD-10 column, the ligated protein was subjected to the modified desulfurization conditions (10 mM 2-nitrobenzylamine hydrochloride salt with 150 mM TCEP, 10 mM VA-044 and 8% (v/v) ^{t}BuSH in 6 M Gdn·HCl, 0.2 M $NaHPO_4$ under nitrogen). To avoid methionine oxidation and nitro reduction, the reaction was cooled to 0 °C, and salts (Gdn·HCl) were rapidly removed after the reaction was completed using a PD-10 column. The crude desulfurized protein was then purified using a HiTrap SP HP cation-exchange column to remove the hydrolyzed thioester α-syn(1−123)OH (Figure S9), followed by activated thiol Sepharose 4B column chromatography, to remove any remaining nondesulfurized proteins (nY125 α-syn A124C) (Figure S10). Characterization of the purified nY125 α-syn by ESI-LC/MS and MALDI-TOF revealed a peak at 14 506 Da (expected mass: 14 505 Da $[M + H]^+$), and neither starting material (nondesulfurized) nor nitro reduced products could be detected (Scheme 3C and Figure S11). The purity of the final product was confirmed by RP-UPLC, which indicated a single peak, and by SDS-PAGE, which revealed a single band at 15kD (Scheme 3, C).

Semisynthesis of α-syn Nitrated at Y39. The semisynthesis of nitrated α-syn at Y39 required the development of a new semisynthetic strategy, because this residue is located in the N-terminal part of the protein. We opted for a three fragment

DOI: 10.1021/ja5131726
J. Am. Chem. Soc. 2015, 137, 5041−5052

Scheme 4. Semisynthesis and Characterization of nY39 α-syn[a]

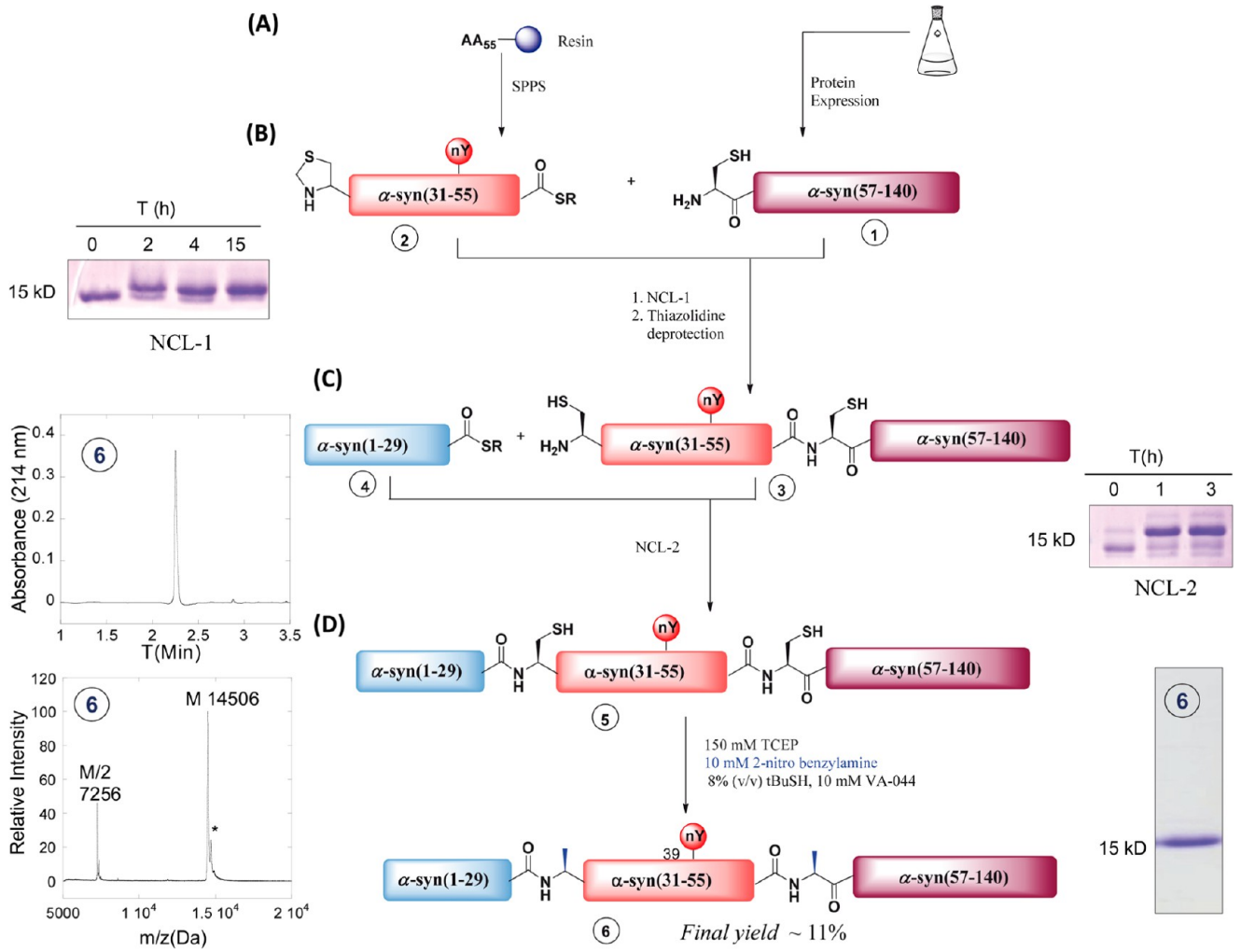

[a](A) One-pot EPL approach used to generate nY39 α-syn. The fragment **1** was recombinantly expressed in *E. coli*. The synthetic peptide **2** was generated by Fmoc-based SPPS. (B) NCL-1, between **1** and **2** and Thz deprotection, SDS-PAGE analysis of the NCL-1 reaction; lanes 1−4 represent the ligation reaction at 0, 2, 4, and 15 h, respectively. (C) NCL-2, between **3** and **4**, SDS-PAGE analysis of the NCL-2 reaction; lanes 1−3 represent the ligation reaction at 0, 1, and 3 h, respectively. (D) Desulfurization of the ligated product **5**, SDS-PAGE, MALDI-TOF, and RP-UPLC analyses of **6** nY39 α-syn (expected mass: 14 506 Da $[M + H]^+$; * corresponds to sinapinic adduct) confirming the purity of the final product.

ligation strategy with the following fragments: α-syn(1−29)SR, **4**; Thz-α-syn(30−55)SR, nY39, **2**; and α-syn(A56C-140)OH, **1** (Scheme S3). The ligation sites were chosen at A29−C30 and V55−C56 (Scheme 2B) based on the availability of alanine residues, which were each mutated to cysteine for the purpose of NCL and then reverted back to native alanine following desulfurization. The N-terminal thioester fragment **4** was obtained by SPPS, and the C-terminal fragment **1** was expressed in *E. coli* and purified as previously described.[35] The middle thioester fragment **2** was synthesized using SPPS with the Cys30 protected as a thiazolidine (Thz). With sufficient quantities of purified fragments **1**, **2**, and **4** (Scheme 4) in hand, we assembled these fragments by two sequential chemical ligations in one pot (Scheme 4A−C), taking advantage of the pH dependence of expressed protein ligation (at pH 7.5) and Thz deprotection (at pH 4.0) (Scheme S4).

The thioester peptide **2** was ligated to recombinant protein **1** at pH 7.5 under reducing and denaturing conditions. The reaction progress was monitored by RP-UPLC and MALDI-TOF (observed mass 11 603 Da, calcd mass 11 606 Da, Figure S14A,B). Next, the Thz group was deprotected by treatment with $MeONH_2$ for 2 h at pH 4 to generate **3** with the requisite free N-terminal Cys. Product formation was confirmed by MALDI-TOF (observed mass 11 594 Da, calcd 11 594 Da, Figure S14C). The pH of the reaction mixture was then increased to 7.5 to perform the final ligation with thioester **4** to generate the full-length protein **5**. The ligation was complete within 3 h, and formation of **5** was monitored by RP-UPLC, and SDS-PAGE gel (Figures S14 and S15) and confirmed by MALDI-TOF (observed mass 14 566 Da, calcd mass 14 570 Da, Figure S14E). Using the desulfurization conditions described above (10 mM 2-nitrobenzylamine hydrochloride salt with 150 mM TCEP, 10 mM VA-044, and 8%(v/v) ^{t}BuSH in 6 M Gdn·HCl, 0.2 M $NaHPO_4$ under nitrogen, Scheme 2D), we achieved efficient and complete desulfurization of both Cys residues to generate pure nY39 α-syn, with minimal nitro reduction (Scheme 4D). The total mass loss of −64 Da from the initial 14 568 Da was monitored over time by ESI-LC/MS (Figure S16). When nitro reduction was first observed, the reaction was immediately cooled to 0 °C, and nY39 α-syn was purified by RP-HPLC using a C18 analytical column,

DOI: 10.1021/ja5131726
J. Am. Chem. Soc. 2015, 137, 5041−5052

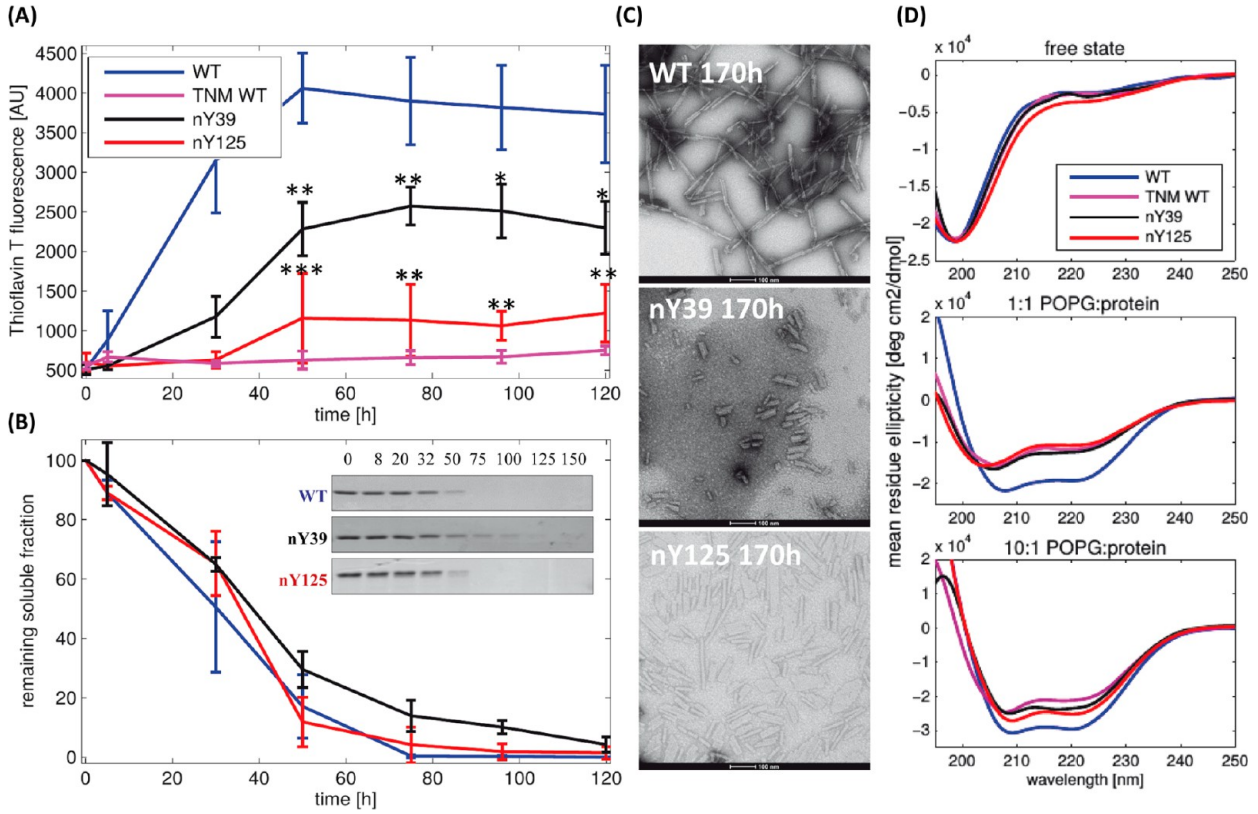

Figure 3. Biophysical characterization: Aggregation, ThT, sedimentation assay, and lipid binding. (A) Aggregation kinetics, based on thioflavin T fluorescence (ThT ± SEM *: p-value <0.05, **: p-value <0.01, ***: p-value <0.001, compared to WT α-syn, $n = 3$). (B) Corresponding quantification of remaining soluble protein ± SEM of recombinant WT and semisynthetic nY39 and nY125 α-syn. The inset shows a representative SDS-PAGE of the remaining soluble protein at different incubation time points. (C) Electron micrographs of recombinant WT α-syn and semisynthetic nY39 and nY125 α-syn. The scale bars are 100 nm. (D) CD of WT, semisynthetic nY39, nY125, and TNM-nitrated α-syn alone or mixed with POPG vesicles at different protein:lipid weight ratios.

which enabled the separation of the desired nY39 α-syn from the 3-amino tyrosine-39 α-syn byproduct and residual cysteine-containing α-syn. The purity and identity of the nY39 protein was assessed by ESI-LC/MS, RP-UPLC, and SDS-PAGE analysis (Scheme 4D and Figure S17).

nY39 and nY125 α-syn Form Fibrils That Are Morphologically Distinct from WT α-syn. Next, we sought to compare the effects of site-specific nitration at Y39 or Y125 on the aggregation properties of α-syn with that of TNM-nitrated and WT α-syn. α-syn is known to spontaneously aggregate into β-sheet-rich lavin T (ThT)-positive fibrils upon incubation at 37 °C with shaking. The kinetics of aggregation, as determined by ThT fluorescence, suggested that WT α-syn aggregates faster and to a greater extent than nY39 or nY125 α-syn (Figure 3A). The ThT signal reached a plateau after 50 h of aggregation in all cases, but the aggregation of both nY125 and nY39 was slightly delayed, with the first increase in ThT values occurring at 50 and 25 h, respectively, compared to 5 h for the WT protein. Moreover, the final absolute ThT plateau signal of the nitrated α-syn was consistently approximately 2- (nY39) and 3-fold (nY125) less than that of the WT. Conversely, and as previously reported,[17,18,20] TNM-nitrated WT α-syn exhibited no increase in ThT signal under these conditions. However, assessment of the aggregation propensity by quantifying the amount of remaining soluble α-syn using the well-established sedimentation assay revealed only slight differences in the aggregation propensities of WT and mononitrated α-syn. As shown in Figure 3B, both nY125 and WT α-syn exhibited a similar pattern of monomer loss, whereas nY39 aggregated slightly slower than both proteins. The sedimentation assay of the TNM-nitrated WT α-syn confirmed the absence of aggregation and revealed a pattern of oligomeric species that did not significantly change with time (Figure S22).

The discrepancy between the ThT and sedimentation assays suggests that the aggregates formed by the mononitrated forms of α-syn may exhibit different structures and ThT binding affinities. To test this hypothesis, we proceeded with assessing the binding of nY39 and nY125 α-syn fibril to Congo Red (CR), another well-established amyloid specific dye that is known to bind to the cross- β-sheet structure of amyloid fibrils. Interestingly, fibrils derived from nY39 and nY125 α-syn did not show significant binding to CR, compared to fibrils prepared from WT α-syn (data not shown). Next, we assessed the structural properties of the aggregates formed by each protein by TEM. TEM images of the fibrils after 170 h (Figure 3C) revealed that WT, nY39, and nY125 α-syn form fibrils with distinct morphologies and size distributions. For both nY39 and nY125 α-syn, the fibrils formed were shorter in length and wider, particularly in the case of nY39. Moreover, the nY125 aggregates exhibited a high propensity to stack in parallel. These morphological distinctions might account for the differences in ThT plateau values observed, because the stacking of fibrils and their structural properties might result in major differences in the number of ThT binding sites.

While WT α-syn readily formed elongated fibrils after 5 h of incubation, both nY39 and nY125 α-syn initially formed

DOI: 10.1021/ja5131726
J. Am. Chem. Soc. 2015, 137, 5041−5052

amorphous aggregates that were converted into short fibrils at longer aggregation times (Figure 4). The presence of predominantly amorphous aggregates in mononitrated samples explains why, despite the slower aggregation kinetics assessed by ThT, the sedimentation assay revealed similar levels of soluble proteins. Indeed, the observed amorphous aggregates are large in size and thus are expected to sediment upon centrifugation. The aggregates formed in the TNM-nitrated WT α-syn sample were also assessed by TEM and revealed the formation of amorphous aggregates but not fibrils. Taken together, these data strongly suggest that nitration at either Y39 or Y125 influences both the aggregation kinetics and the structure of α-syn aggregates, whereas a mixture of dityrosine cross-links and nitration at all four tyrosine residues leads to the formation of predominantly oligomeric species and blocks α-syn fibril formation (Figure 4).

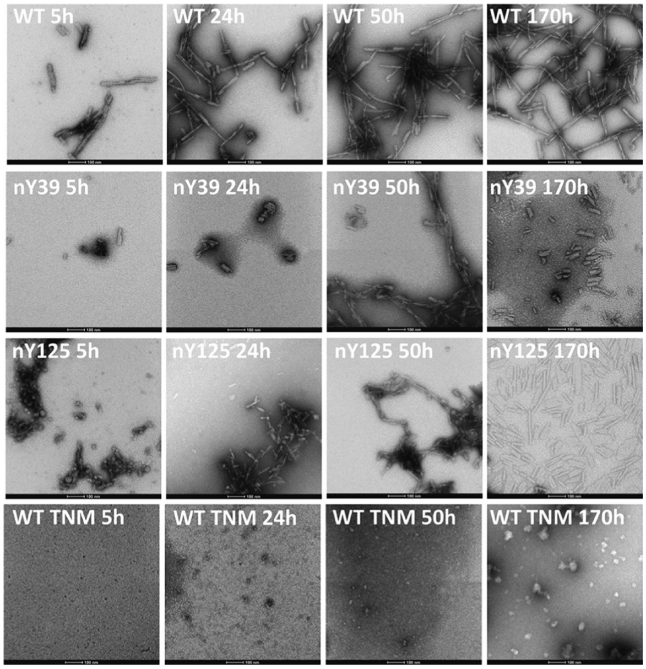

Figure 4. Time-dependent aggregation of WT and nitrated α-syn followed by TEM. Electron micrographs of recombinant WT, semisynthetic nY39, nY125, and TNM-nitrated WT α-syn. The scale bars are 100 nm.

nY39 and nY125 α-syn Exhibit Reduced Affinity to Negatively Charged Vesicles Compared to WT α-syn. The interaction of α-syn with lipid bilayers at the presynaptic terminal is known to play a key role in regulating α-syn oligomerization and its function in SNARE complex assembly and neurotransmission.[36−39] We investigated the effects of mononitration on the propensity of α-syn α-helix formation upon binding to negatively charged POPG vesicles, in comparison with TNM-nitrated WT protein. WT, nY39, nY125, or TNM-nitrated WT α-syn were mixed with POPG vesicles at various ratios (1:0, 1:0.5, 1:1, 1:5, and 1:10, w/w) and protein secondary structure was assessed by circular dichroism (CD). As shown in Figures 3D and S23 and consistent with previous reports, we observed an increase in WT α-syn α-helical content with increasing POPG ratio. Both mononitrated α-syn (nY39 and nY125) and the TNM-nitrated WT protein exhibited a slight reduction in α-helical propensity in the presence of vesicles. These results are in agreement with a previous study of nitrated α-syn mutant (Y125/133/136F), which demonstrated that the presence of a partially negative group at residue Y39 induced a decreased binding to negatively charged vesicles, due to electrostatic repulsion.[21] The similar decrease in vesicle binding by the C-terminal Y125 may seem surprising because this residue is not located in the membrane-binding region of α-syn. However, the same study demonstrated that this decrease in membrane binding is not due to electrostatic repulsion, but rather due to a change in the α-syn conformation that alters long-range interactions between the N- and C-terminal regions of the protein.[19,21] Together, these results suggest that nitration at the N- or C-terminal regions results in a slight but significant reduction in helix formation upon α-syn membrane binding.

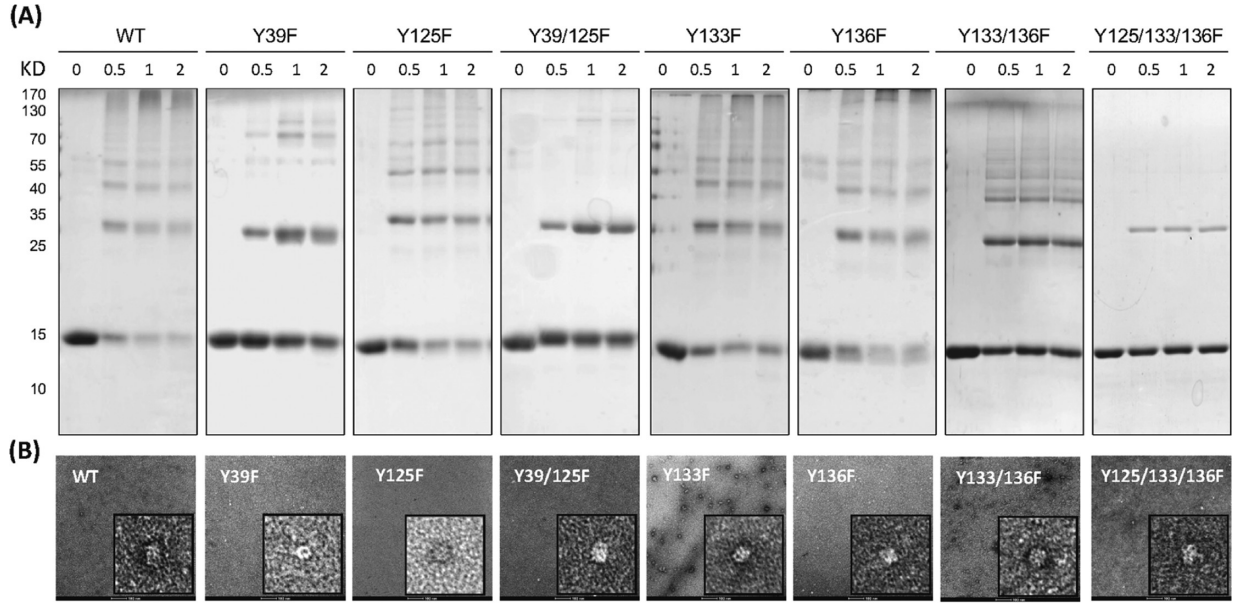

Figure 5. Nitration of α-syn mutants by TNM. (A) SDS-PAGE analysis of the nitration reactions of mutant α-syn. Lanes 1−4 represent the reaction after 0, 0.5, 1, and 2 h, respectively. (B) Electron micrographs of recombinant nitrated WT and mutant α-syn. The scale bars are 100 nm.

DOI: 10.1021/ja5131726
J. Am. Chem. Soc. 2015, 137, 5041−5052

The Number and Position of Tyrosine Residues Determine the Nitration-Induced Oligomerization Profile of α-syn. Because both nitration and o-o′-dityrosine cross-linked forms of α-syn have been detected in brain lesions of PD patients, we sought to determine which tyrosine residues are involved in o-o′-dityrosine formation and to assess their relative roles in α-syn nitration and oligomerization. Thus, we generated a series of α-syn mutants in which single or multiple tyrosine residues were mutated to phenylalanine (Y39F, Y125F, Y133F, Y136F, Y39/125F, Y133/136F and Y125/133/136F), which is inert to nitration. TNM was used to nitrate the α-syn mutants, and the nitration was monitored by SDS-PAGE and ESI-LC/MS to ensure complete nitration of the available tyrosine residues in α-syn (Figures 5, S18, and S19). Interestingly, nitration of the different mutated forms of α-syn produced unique heterogeneous profiles of nitrated monomers and cross-linked dimers, trimers, and higher molecular weight (HMW) oligomers.

When no tyrosines (WT) or any of the three C-terminal tyrosine residues were mutated (Y125F, Y133F, or Y136F), we observed a rapid depletion of monomers and the predominant formation of dimers and HMW species upon TMN treatment. In these cases, dityrosine formation can occur between the Y39 and any of the remaining C-terminal tyrosine residues, thus favoring the formation of higher-order cross-linked oligomers (Figure 6B). Conversely, analysis of TNM-treated Y39F sample revealed the presence of predominantly α-syn monomers and dimers and only a small amount of higher order oligomers. These results suggest that nitration of Y39 and dityrosine formation involving this residue both play a critical role in the oligomerization of α-syn. When Y39 is mutated, tyrosine cross-linking can only occur between the C-terminal tyrosine residues. The close proximity of these residues (Y125, Y133, Y136) may interfere with the occurrence of multiple dityrosine cross-linking due to steric hindrance (Figure 6D), thus interfering with the formation of higher order aggregates. The double band observed around the dimeric specie (approximately 35 kDa) could be due to the variability in cross-linking sites, thus resulting in dimers with different conformations. Interestingly, when both Y39 and Y125 were mutated, we observed a significant reduction in the formation of HMW species and increased levels of dimers and monomers. Finally, when all three C-terminal tyrosine residues were mutated (Y125F/133F/136F), mostly monomers and some dimers were formed, but no oligomers were observed (Figure 5A).

Overall, we observe that when Y39 is not available for nitration (Y39F and Y39/125F), the extent of cross-linking is limited mostly to dimer formation, while mutants in which Y39 is still available, along with one or multiple C-terminal tyrosines (Y125F, Y133F, Y136F and Y133/136F), readily form higher order oligomers. The extent of oligomer formation tends to decrease with the reduction of the number of available C-terminal tyrosine residues.

To elucidate the role of the N-terminal region of α-syn in regulating the nitration of C-terminal tyrosine residues, we nitrated the peptide fragment α-syn (129−140) using TNM. Interestingly, we observed nitration of the tyrosine residues, but no dimer or HMW species were detected by ESI-LC/MS (Figure S21). Similarly, when we nitrated N-terminally truncated α-syn (71−140) using the exact same conditions used to nitrate WT-α-syn, we also solely observed nitration and no oligomer formation (Figure S21). This result suggests that the N-terminal region of the protein (1−70) plays a role in TMN-induced dityrosine bond formation, possibly by favoring intramolecular interactions that expose the tyrosine residues to the cross-linking reaction and/or by favoring intermolecular interactions, bringing α-syn monomers in close proximity and allowing cross-linking between two α-syn proteins.

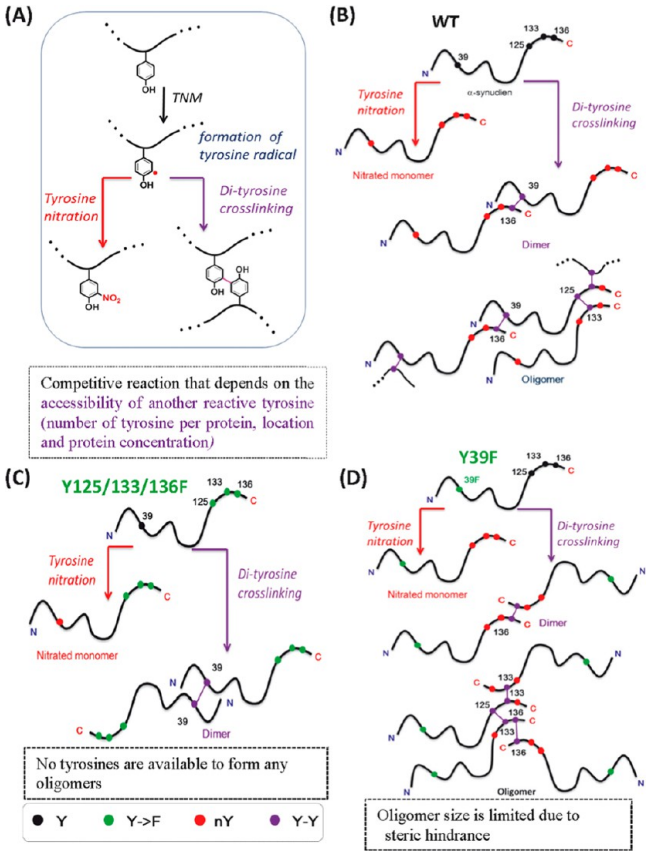

Figure 6. Schematic depiction summarizing our results and working model on the role of nitration in regulating α-syn oligomerization and dityrosine formation. (A) TNM induces the formation of reactive tyrosines, which either become nitrated or form dityrosine cross-links. (B) In the case of WT α-syn, the formation of multiple dityrosine bonds is favored because tyrosine residues are available at both ends of the protein. (C) Y125/133/136F α-syn can either undergo nitration or cross-linking; cross-link is limited to dimer formation. (D) In Y39F α-syn, the tyrosine residues are clustered in the C-terminal region of the protein, and thus oligomer size is limited due to steric hindrance, while dimer formation is favored.

TEM images of the nitrated WT and C-terminal tyrosine mutants revealed the formation of small oligomeric species (Figure 5B), in agreement with the observation of oligomers by SDS PAGE. Interestingly, the mutants containing a phenylalanine at position 133 exhibited larger oligomers. This suggests that the absence of cross-linking at this residue affects the conformation of the oligomers, resulting in the differing morphologies observed by TEM. Surprisingly, we also observed oligomer formation in the cases of the Y39 (Y39F and Y39/125F) and the Y125/133/136F mutants. This was unexpected because cross-linking is mostly limited to the formation of dimers, which are too small to be observed by TEM. However, it is possible that the dimers form noncovalent interactions with each other, leading to the formation of larger species that can be detected by TEM, or that the relative amount of these oligomers is very small but still detectable by TEM.

Differences in Oligomeric Species Distribution Between the TNM-Nitrated Mutants Are Explained by

DOI: 10.1021/ja5131726
J. Am. Chem. Soc. 2015, 137, 5041−5052

Tyrosine Availability, Steric Hindrance, and Competition with Nitration. Based on our results and on those reported by others, we propose the following model for the role of nitration in regulating α-syn oligomerization (Figure 6). TNM induces the formation of reactive tyrosines, which either become nitrotyrosines or form dityrosine bonds with other reactive tyrosines (Figure 6A). These two reactions are in competition, and the outcome depends mainly on the availability of reactive tyrosines, which will favor dityrosine cross-linking, because of the increased probability that the two tyrosines will be in close proximity and thus to react with each other. The availability of tyrosines themselves depends on the sample concentration, the number of tyrosines per protein, and the location of the tyrosine residues. To test this hypothesis, we performed TNM nitration with increasing α-syn concentrations, while the TNM amount was kept constant. As expected, we observed depletion of monomeric tetra-nitrated α-syn and an increase in HMW species with increasing α-syn concentration. Interestingly, at 400 μM α-syn, we observed mostly HMW oligomers (Figure S20A). Notably, reducing the concentration of TNM while keeping the protein concentration constant did not yield the same pattern. This is easily explained by the requirement for excess TNM to activate tyrosine residues either for nitration or cross-linking (Figure S20B). Clusters of tyrosine residues in close proximity limits the extent of cross-linking, most likely due to steric hindrance. For WT α-syn, which contains a total of four tyrosine residues in both the C- and N-terminal regions, multiple dityrosine-bond formation is highly favored, because the probability that at least two residues per protein undergo cross-linking before nitration is high. Because tyrosine residues are available at both ends of the protein, an increased probability of intermolecular cross-linking events is not surprising. This leads to the formation of a high proportion of HMW oligomer species at the expense of tetra-nitrated monomeric and LMW oligomeric species, such as dimers and trimers (Figure 6B). Mutants with one or two Y → F mutations in the C-terminal region of the protein exhibit behavior similar similar to that of the WT protein, because the N- and C-terminal tyrosine residues are still available and engage in intermolecular cross-linking. However, the reduction in the absolute number of available tyrosine residues decreases the probability of tyrosine cross-linking before the nitration reaction and thus limits the proportion of HMW species. Conversely, a strong decrease in the proportion of HMW species is observed when the only N-terminal tyrosine residue (Y39) is mutated because steric hindrance limits the number of C-terminal cross-linking reactions (Figure 6D), thus favoring the formation of nitrated monomers and dityrosine dimers. If a C-terminal residue is also mutated, the effect is even stronger, as observed for the Y39/125F mutant. Finally, when a single tyrosine residue remains, as is in Y125/133/136F α-syn, oligomers cannot form, and only monomers and dimers are observed (Figure 6C).

Trypsin-digestion of dimeric α-syn confirms covalent dityrosine cross-linking between the two tyrosine residues. A previous characterization of α-syn dityrosine cross-linking characterization, based on the acidic hydrolysis of oligomers followed by HPLC purification, reported a dityrosine peak along with the nitrotyrosine and tyrosine peaks,[20] thus providing direct evidence for dityrosine bond formation. To identify the residues involved in dityrosine formation, we characterized the dimers formed by Y39/125F α-syn, which was selected because this mutant forms predominantly dimers involving C-terminal Y133 or Y136 residues in three possible ways (Y133:Y133, Y133:Y136, and Y136:Y136, Figures 7A–C,

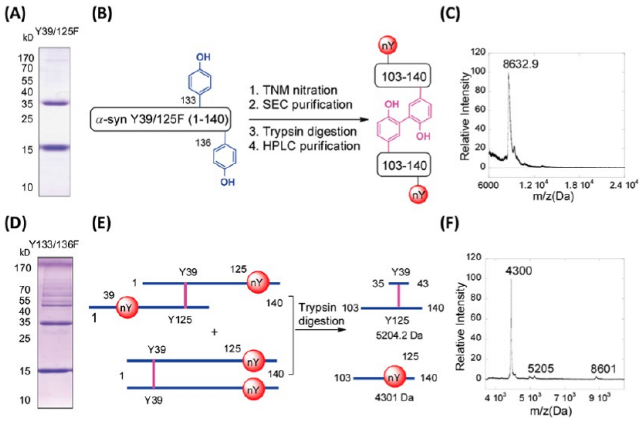

Figure 7. α-syn dimer characterization. (A) SDS-PAGE analysis of the nitration reaction of Y39/125F α-syn. (B) Schematic diagram of dimer characterization process. (C) MALDI-TOF analysis of purified digested protein dimer, expected mass 8632.8 Da for $[M + H]^+$. (D) SDS-PAGE analysis of the nitration reaction of Y133/136F α-syn. (E) MALDI-TOF analysis of trypsin-digested Y133/136F α-syn dimer, expected mass 4301 and 5204.2 Da for $[M + H]^+$. (F) Expected tryptic digested fragment cross-linked at Y39:Y125 and fragment cross-linked Y39:Y39.

S24, and S25). To determine the specific residues involved in dityrosine formation, we first purified the Y39/125F α-syn cross-linked dimer from the TNM nitration reaction by SEC. The purified dimers were then subjected to trypsin digestion because this procedure leaves the C-terminus intact and generates a smaller fragment (~8 kD, corresponding to the cross-linked dimer (N103–A140). We were unable to detect the 8 kD band by SDS-PAGE, native gel, immunoblots using a variety of C-terminal antibodies and by ESI-LC/MS remained unsuccessful (data not shown), most likely due to the highly negative C-terminal fragment generated, which does not migrate on gels and fails to ionize in MS. Indeed, to the best of our knowledge, no one has reported a protocol for SDS-PAGE-based detection of C-terminal fragments of α-syn. We therefore purified the trypsin-digested protein by analytical RP-HPLC. MALDI-TOF analysis revealed a peak at 8632.9 Da, which matches with the expected mass 8632.8 Da for a cross-linked C-terminal fragment encompassing residues (Y133:Y133, Y133:Y136, or Y136:Y136) (Figure 7C).

We next characterized dimers of Y133/136F α-syn to determine whether dityrosine formation could occurred between the Y125 and Y39 residues. MALDI-TOF analysis of the trypsin digested purified dimer revealed a small peak at 5205 Da corresponding to the cross-linking of the N-terminal α-syn (35×10^{-43} K) and C-terminal α-syn (103×10^{-140} A) peptides through Y39–Y125 residues between two monomers and a major peak at 4300 Da, which corresponds to the digested product of the Y39–Y39 cross-linked proteins (Figure 7D–F).

Nitration Does Not Block Phosphorylation at S129 *in Vitro*. The majority of α-syn in LBs is phosphorylated at S129, and phosphorylation at this residue has emerged as an important pathological marker in PD and animal models of synucleinopathies. Several lines of evidence suggest that S129 phosphorylation plays an important role in regulating α-syn membrane binding,[40] subcellular localization,[41] ubiquitination,[42] turnover,[43] aggregation,[44] and metal binding.[45] Since S129 is located between tyrosine residues Y125 and Y133 of α-syn, we sought to assess the influence of nitration at single or multiple tyrosine residues on S129 phosphorylation. To probe the cross-talk between tyrosine nitration and phosphorylation at S129, we

DOI: 10.1021/ja5131726
J. Am. Chem. Soc. 2015, 137, 5041–5052

determined the relative effect of nitration at several residues on PLK3 kinase-mediated phosphorylation at S129. PLK3 is a member of the serine family of kinases and, like PLK2, has been shown to interact with and efficiently phosphorylate α-syn at S129 *in vitro* and in cell culture.[46] Phosphorylation at S129 was detected using mouse monoclonal anti-pS129 α-syn (from Wako) (Figure 8A–C) and confirmed by MALDI-TOF analysis

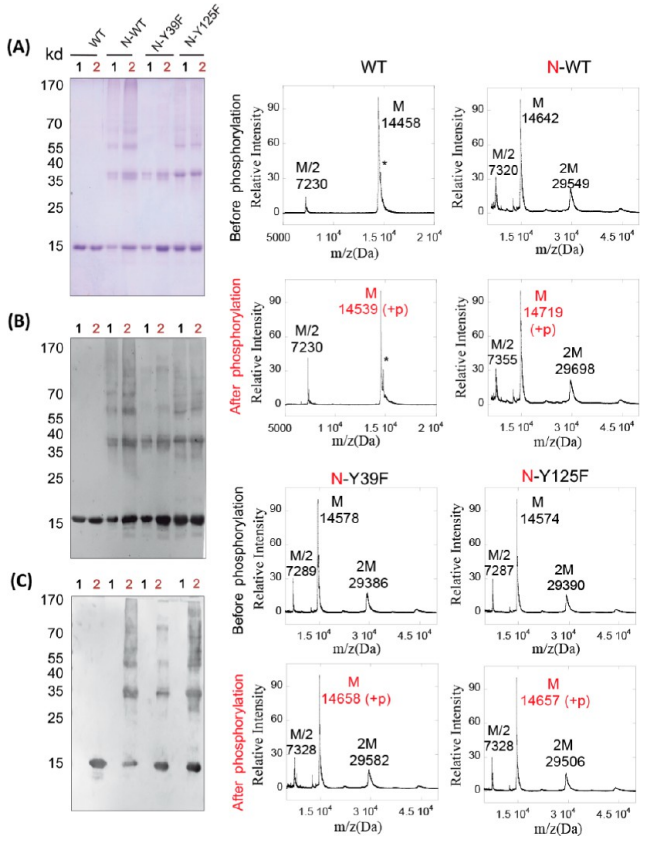

Figure 8. *In vitro* phosphorylation of nitrated α-syn by PLK3. (A) SDS-PAGE and (B) immunoblot probed with total or (C) pS129 α-syn antibodies to assess the phosphorylation reaction of nitrated α-syn. Lanes 1 and 2 represent before and after the reaction. (D) MALDI-TOF analyses before and after the phosphorylation reaction.

(Figure 8D). In all cases, MALDI-TOF analysis indicated efficient phosphorylation, with the desired +80 Da ($-PO_3H_2$) increase from the initial mass. These results indicate that nitration of α-syn at any tyrosine residue does not prevent recognition of the protein by PLK3 and does not affect its subsequent phosphorylation at S129. Interestingly, PLK3 also phosphorylates cross-linked, nitrated dimers, trimers, and HMW oligomers. These results strongly suggest that nitration in the C- or N-terminal region does not significantly affect PLK3-mediated phosphorylation *in vitro*.

N-Terminal α-syn Antibodies Strongly Detect Oligomers of TNM-Nitrated WT and α-syn Mutants. To investigate the effects of nitration and cross-linking on α-syn conformation, we used a panel of anti-α-syn antibodies to assess the accessibility of different regions of nitrated WT and Y → F mutants of α-syn after nitration. The epitopes of the antibodies are shown in Figure S26A. Strikingly, all N-terminal antibodies screened exhibited stronger preference for recognizing the oligomeric species than the monomer (Figure S26C, top panel), and no differences in the distribution of oligomeric species were detected by any of the antibodies screened (Figure S26C). These results suggest that N-terminal recognition is favored by cross-linking, possibly due to conformational changes favoring antibody binding. Interestingly, for all the proteins analyzed, the antibody Ab5336P recognized monomeric and dimeric species more strongly than the higher oligomeric species. This suggests that residues within the 108–120 region become less accessible in the dityrosine-cross-linked oligomers. When the antibody recognition epitope is away from N- or C-terminal cross-linking sites, as in the case of antibodies Fl-140 and Syn-1, they recognize all monomeric, dimeric, and higher oligomeric species. As expected, all proteins in which Y125 is mutated, nitrated, or cross-linked were poorly detected by the antibody SC211. In summary, these data suggests that the cross-linked α-syn species have a more open conformation in the N-terminal region compared to the monomeric species.

CONCLUSION

Using native chemical ligation combined with a novel desulfurization strategy, we were able to achieve site-specific incorporation of 3-NT in α-syn for the first time. This is the first example of the preparation of site-specifically nitrated proteins using protein semisynthesis. The key to this achievement was the discovery that treatment with 2-nitrobenzyl HCl suppressed nitro-group reduction during desulfurization to a degree sufficient to obtain site-specifically nitrated proteins in milligram quantities. Using this method, we generated site-specific nY39 and nY125 α-syn corresponding to pathologically relevant nitration sites of α-syn. In contrast to nonspecifically TNM-nitrated α-syn, both of these site-selective nitrated proteins could be aggregated to form fibrils with distinct structures and morphologies. The slightly lower affinity to negatively charged membranes previously reported for TNM-nitrated α-syn[19] was also observed for the site-specifically nitrated proteins. We also demonstrated that nitration has no effect on the phosphorylation of S129 by PLK3 and that recognition by several antibodies is affected both by nitration and dityrosine cross-linking, most likely due to changes in conformation, epitope exposure and availability. Analysis of the TNM nitration pattern and cross-linking profiles of a library of Y → F mutated α-syn proteins revealed that the presence of both C- and N-terminal tyrosines is essential for the formation of HMW oligomers. In addition, nitration and oligomer patterns are strongly dependent on the competition between nitration and cross-linking and are influenced by the intramolecular conformations, the protein concentration, the number of tyrosine residues per protein, and their locations within the protein. Our semisynthetic strategy for generating site-specifically nitrated proteins opens new opportunities for assessing the role of nitration in regulating protein structure and function in health and disease.

ASSOCIATED CONTENT

Supporting Information

Description of material and methods, experimental details, purification procedures, protein characterization, and supplemental data included. This material is available free of charge via the Internet at http://pubs.acs.org.

AUTHOR INFORMATION

Corresponding Author

*hilal.lashuel@epfl.ch

DOI: 10.1021/ja5131726
J. Am. Chem. Soc. 2015, 137, 5041–5052

Notes

The authors declare no competing financial interest.

■ ACKNOWLEDGMENTS

The authors wish to acknowledge Nathalie Jordan for preparation of all the plasmids, Dr. Bruno Fauvet for helping in aggregation studies and discussions, Dr. Sean Michael Deguire and Dr. John Warner for reviewing the manuscript, Dr. Adrian Schmid and Dr. Marc Moniatte for assistance with dimer characterization from EPFL proteomics core facility. This work was funded by grants from the Swiss National Science Foundation (315230-125483), the European Research Council starting grant (243182), and the Micahel J Fox Foundation.

■ REFERENCES

(1) McCormack, A. L.; Mak, S. K.; Di Monte, D. A. *Cell. Death Dis.* **2012**, *3*, e315.
(2) Jenner, P. *Ann. Neurol.* **2003**, *53* (Suppl 3), S26.
(3) Schildknecht, S.; Gerding, H. R.; Karreman, C.; Drescher, M.; Lashuel, H. A.; Outeiro, T. F.; Di Monte, D. A.; Leist, M. *J. Neurochem.* **2013**, *125*, 491.
(4) Beckman, J. S.; Beckman, T. W.; Chen, J.; Marshall, P. A.; Freeman, B. A. *Proc. Natl. Acad. Sci. U.S.A.* **1990**, *87*, 1620.
(5) Beckman, J. S.; Crow, J. P. *Biochem. Soc. Trans.* **1993**, *21*, 330.
(6) Radi, R. *Proc. Natl. Acad. Sci. U.S.A.* **2004**, *101*, 4003.
(7) Duda, J. E.; Giasson, B. I.; Chen, Q.; Gur, T. L.; Hurtig, H. I.; Stern, M. B.; Gollomp, S. M.; Ischiropoulos, H.; Lee, V. M.; Trojanowski, J. Q. *Am. J. Pathol.* **2000**, *157*, 1439.
(8) Giasson, B. I.; Duda, J. E.; Murray, I. V.; Chen, Q.; Souza, J. M.; Hurtig, H. I.; Ischiropoulos, H.; Trojanowski, J. Q.; Lee, V. M. *Science* **2000**, *290*, 985.
(9) Fernandez, E.; Garcia-Moreno, J. M.; Martin de Pablos, A.; Chacon, J. *Antioxid. Redox. Sign.* **2013**, *19*, 912.
(10) Prigione, A.; Piazza, F.; Brighina, L.; Begni, B.; Galbussera, A.; Difrancesco, J. C.; Andreoni, S.; Piolti, R.; Ferrarese, C. *Neurosci. Lett.* **2010**, *477*, 6.
(11) Liu, Y.; Qiang, M.; Wei, Y.; He, R. *J. Mol. Cell. Biol.* **2011**, *3*, 239.
(12) Yu, Z.; Xu, X.; Xiang, Z.; Zhou, J.; Zhang, Z.; Hu, C.; He, C. *PLoS One* **2010**, *5*, e9956.
(13) Reynolds, A. D.; Glanzer, J. G.; Kadiu, I.; Ricardo-Dukelow, M.; Chaudhuri, A.; Ciborowski, P.; Cerny, R.; Gelman, B.; Thomas, M. P.; Mosley, R. L.; Gendelman, H. E. *J. Neurochem.* **2008**, *104*, 1504.
(14) Paxinou, E.; Chen, Q.; Weisse, M.; Giasson, B. I.; Norris, E. H.; Rueter, S. M.; Trojanowski, J. Q.; Lee, V. M.; Ischiropoulos, H. *J. Neurosci.* **2001**, *21*, 8053.
(15) Norris, E. H.; Giasson, B. I.; Ischiropoulos, H.; Lee, V. M. *J. Biol. Chem.* **2003**, *278*, 27230.
(16) Stone, D. K.; Kiyota, T.; Mosley, R. L.; Gendelman, H. E. *Neurosci. Lett.* **2012**, *523*, 167.
(17) Uversky, V. N.; Yamin, G.; Munishkina, L. A.; Karymov, M. A.; Millett, I. S.; Doniach, S.; Lyubchenko, Y. L.; Fink, A. L. *Mol. Brain Res.* **2005**, *134*, 84.
(18) Yamin, G.; Uversky, V. N.; Fink, A. L. *FEBS Lett.* **2003**, *542*, 147.
(19) Hodara, R.; Norris, E. H.; Giasson, B. I.; Mishizen-Eberz, A. J.; Lynch, D. R.; Lee, V. M.; Ischiropoulos, H. *J. Biol. Chem.* **2004**, *279*, 47746.
(20) Souza, J. M.; Giasson, B. I.; Chen, Q.; Lee, V. M.; Ischiropoulos, H. *J. Biol. Chem.* **2000**, *275*, 18344.
(21) Sevcsik, E.; Trexler, A. J.; Dunn, J. M.; Rhoades, E. *J. Am. Chem. Soc.* **2011**, *133*, 7152.
(22) Benner, E. J.; Banerjee, R.; Reynolds, A. D.; Sherman, S.; Pisarev, V. M.; Tsiperson, V.; Nemachek, C.; Ciborowski, P.; Przedborski, S.; Mosley, R. L.; Gendelman, H. E. *PLoS One* **2008**, *3*, e1376.
(23) Krishnan, S.; Chi, E. Y.; Wood, S. J.; Kendrick, B. S.; Li, C.; Garzon-Rodriguez, W.; Wypych, J.; Randolph, T. W.; Narhi, L. O.; Biere, A. L.; Citron, M.; Carpenter, J. F. *Biochemistry* **2003**, *42*, 829.
(24) Neumann, H.; Hazen, J. L.; Weinstein, J.; Mehl, R. A.; Chin, J. W. *J. Am. Chem. Soc.* **2008**, *130*, 4028.
(25) Danielson, S. R.; Held, J. M.; Schilling, B.; Oo, M.; Gibson, B. W.; Andersen, J. K. *Anal. Chem.* **2009**, *81*, 7823.
(26) Hejjaoui, M.; Butterfield, S.; Fauvet, B.; Vercruysse, F.; Cui, J.; Dikiy, I.; Prudent, M.; Olschewski, D.; Zhang, Y.; Eliezer, D.; Lashuel, H. A. *J. Am. Chem. Soc.* **2012**, *134*, 5196.
(27) Fauvet, B.; Fares, M. B.; Samuel, F.; Dikiy, I.; Tandon, A.; Eliezer, D.; Lashuel, H. A. *J. Biol. Chem.* **2012**, *287*, 28243.
(28) Haj-Yahya, M.; Fauvet, B.; Herman-Bachinsky, Y.; Hejjaoui, M.; Bavikar, S. N.; Karthikeyan, S. V.; Ciechanover, A.; Lashuel, H. A.; Brik, A. *Proc. Natl. Acad. Sci. U.S.A.* **2013**, *110*, 17726.
(29) Wissner, R. F.; Batjargal, S.; Fadzen, C. M.; Petersson, E. J. *J. Am. Chem. Soc.* **2013**, *135*, 6529.
(30) Metanis, N.; Keinan, E.; Dawson, P. E. *Angew. Chem., Int. Ed.* **2010**, *49*, 7049.
(31) Wu, B.; Chen, J.; Warren, J. D.; Chen, G.; Hua, Z.; Danishefsky, S. J. *Angew. Chem., Int. Ed.* **2006**, *118*, 4222.
(32) Liu, P.; O'Mara, B. W.; Warrack, B. M.; Wu, W.; Huang, Y.; Zhang, Y.; Zhao, R.; Lin, M.; Ackerman, M. S.; Hocknell, P. K.; Chen, G.; Tao, L.; Rieble, S.; Wang, J.; Wang-Iverson, D. B.; Tymiak, A. A.; Grace, M. J.; Russell, R. J. *J. Am. Soc. Mass Spectrom.* **2010**, *21*, 837.
(33) Muir, T. W.; Sondhi, D.; Cole, P. A. *Proc. Natl. Acad. Sci. U.S.A.* **1998**, *95*, 6705.
(34) Dang, B.; Kubota, T.; Mandal, K.; Bezanilla, F.; Kent, S. B. H. *J. Am. Chem. Soc.* **2013**, *135*, 11911.
(35) Fauvet, B.; Butterfield, S. M.; Fuks, J.; Brik, A.; Lashuel, H. A. *Chem. Commun.* **2013**, *49*, 9254.
(36) Fortin, D. L.; Troyer, M. D.; Nakamura, K.; Kubo, S.; Anthony, M. D.; Edwards, R. H. *J. Neurosci.* **2004**, *24*, 6715.
(37) Davidson, W. S.; Jonas, A.; Clayton, D. F.; George, J. M. *J. Biol. Chem.* **1998**, *273*, 9443.
(38) Perrin, R. J.; Woods, W. S.; Clayton, D. F.; George, J. M. *J. Biol. Chem.* **2000**, *275*, 34393.
(39) Murphy, D. D.; Rueter, S. M.; Trojanowski, J. Q.; Lee, V. M. *J. Neurosci.* **2000**, *20*, 3214.
(40) Visanji, N. P.; Wislet-Gendebien, S.; Oschipok, L. W.; Zhang, G.; Aubert, I.; Fraser, P. E.; Tandon, A. *J. Biol. Chem.* **2011**, *286*, 35863.
(41) Lee, B. R.; Matsuo, Y.; Cashikar, A. G.; Kamitani, T. *J. Cell Sci.* **2013**, *126*, 696.
(42) Hasegawa, M.; Fujiwara, H.; Nonaka, T.; Wakabayashi, K.; Takahashi, H.; Lee, V. M.; Trojanowski, J. Q.; Mann, D.; Iwatsubo, T. *J. Biol. Chem.* **2002**, *277*, 49071.
(43) Oueslati, A.; Schneider, B. L.; Aebischer, P.; Lashuel, H. A. *Proc. Natl. Acad. Sci. U.S.A.* **2013**, *110*, E3945.
(44) Paleologou, K. E.; Schmid, A. W.; Rospigliosi, C. C.; Kim, H. Y.; Lamberto, G. R.; Fredenburg, R. A.; Lansbury, P. T., Jr.; Fernandez, C. O.; Eliezer, D.; Zweckstetter, M.; Lashuel, H. A. *J. Biol. Chem.* **2008**, *283*, 16895.
(45) Lu, Y.; Prudent, M.; Fauvet, B.; Lashuel, H. A.; Girault, H. H. *ACS Chem. Neurosci.* **2011**, *2*, 667.
(46) Mbefo, M. K.; Paleologou, K. E.; Boucharaba, A.; Oueslati, A.; Schell, H.; Fournier, M.; Olschewski, D.; Yin, G.; Zweckstetter, M.; Masliah, E.; Kahle, P. J.; Hirling, H.; Lashuel, H. A. *J. Biol. Chem.* **2010**, *285*, 2807.

DOI: 10.1021/ja5131726
J. Am. Chem. Soc. 2015, 137, 5041−5052